ELSEVIER

Biochimica et Biophysica Acta 1323 (1997) 154–162

BIOCHIMICA ET BIOPHYSICA ACTA
BBA

Amphiphilic sites for general anesthetic action? Evidence from ^{129}Xe-{^{1}H} intermolecular nuclear Overhauser effects

Yan Xu [a,b,*], Pei Tang [a]

[a] *Department of Anesthesiology and Critical Care Medicine, University of Pittsburgh, Pittsburgh, PA 15261, USA*
[b] *Department of Pharmacology, University of Pittsburgh, Pittsburgh, PA 15261, USA*

Received 8 May 1996; accepted 21 August 1996

Abstract

Because a strong correlation exists between the potency of general anesthetics and their ability to dissolve in oil, a lipophilic site of action is often assumed. We show here that a lipophilic molecule may preferentially target less lipophilic sites after interaction with a membrane takes place. Xenon, a chemically inert and structureless general anesthetic, was chosen as an unbiased molecular probe for assessment of its dynamic distribution. Site-selective, intermolecular ^{129}Xe-{^{1}H} nuclear Overhauser effects were used to measure the specific interaction between xenon and protons in different regions in a phosphatidylcholine lipid membrane. It was evident that xenon–membrane interaction was directed toward the amphiphilic head region, with significant involvement of interfacial water, despite xenon's apolar and highly lipophilic nature in the gas phase. This result may suggest the importance of amphiphilicity in association with anesthetic action.

Keywords: Anesthetic, xenon; Xenon; Lipid–anesthetic interaction; Mechanisms of general anesthesia; Nuclear magnetic resonance (NMR); NMR; Nuclear Overhauser effect (NOE)

1. Introduction

It remains a great scientific challenge to determine the molecular mechanisms of general anesthesia. From practitioners to experimentalists and theorists, the thinking has been directed to one of the two putative target sites: the lipid portion of neuronal membranes [1–8] or the hydrophobic pockets in certain crucial excitable proteins [9–13]. Irrespective of lipids or proteins, it is often assumed that the site of action is hydrophobic in nature. This assumption is based primarily on the key observations, made by Meyer [14] and Overton [15] at the turn of century, that the potency of general anesthetics correlates strongly with their solubility in organic solvents, such as olive oil (the Meyer–Overton rule). More recently, a similarly successful correlation has been observed in a lipid-free soluble protein, firefly luciferase [16], supporting the idea that the hydrophobic site can be modeled by a protein.

Deviation from the Meyer–Overton rule, however, has been observed. For instance, in homologous series of alkanols [17,18] and alkanes [19–21], potency increases with molecular weight until a point where potency is suddenly and unexpectedly lost, despite the 'favorable' oil solubility of the larger members. This cutoff phenomenon was originally thought to relate to molecular size [18,22], or to slow uptake and equilibration of the larger members at the site(s) of

* Corresponding author at: W-1358 Biomedical Science Tower, University of Pittsburgh, Pittsburgh, PA 15261, USA. Fax: +1 (412) 6489587; E-mail: xu2+@pitt.edu

PII S0005-2736(96)00184-8

action [23,24]. More recent studies [19–21,25] have revealed that some molecules, strikingly resembling potent general anesthetics, are completely devoid of anesthetic effects [21]. Neither hydrophobicity nor pharmacokinetics can account for the difference [21,26].

Determination of the cause of such discrepancy may help to identify the sites of general anesthetic action and thereby shed new light on the molecular mechanisms of general anesthesia [21,27]. It has been suggested [21] that a site affected by both anesthetic and nonanesthetic agents is unlikely to be relevant to the production of anesthesia, whereas that corresponding to correct physiological responses has an increased chance to be involved in anesthesia.

However, other than their clinical effects, anesthetics and nonanesthetics are undefined at the molecular level. We contend that if a set of molecular properties can be used to differentiate the anesthetic molecules as a group from the nonanesthetic, then these properties must be either maintained or assumed after interaction with the relevant sites takes place. We further hypothesize that such interaction may alter the preferential selection of a molecule for different molecular target sites. To prove that such selection indeed occurs and to examine the dynamic distribution of a molecule in different molecular environments, investigations are needed that directly characterize specific interaction between an anesthetic (or a nonanesthetic) and a biological macromolecule, without limiting to the traditional concept of solubility in a bulk phase. We report here such an investigation using nuclear magnetic resonance (NMR) spectroscopy. Intermolecular, heteronuclear, ^{129}Xe-{^{1}H} nuclear Overhauser effects (NOE) were used to measure the site-specific interaction between xenon, a clinical general anesthetic [28–32], and a phosphatidylcholine (PC) lipid membrane. Results from this investigation have been presented in part in form of abstracts previously [33–35].

2. Materials and methods

2.1. Sample preparation

Because they contain simultaneously lipophilic, hydrophilic, and amphiphilic regions and can be easily quantified by NMR, liquid suspensions of protein-free PC vesicles, containing 0–50% cholesterol (in molar ratio), were used as a model system in this study. To prepare the vesicles, a procedure similar to that of Smith et al. [36] was used. Briefly, measured amounts of dry L-α-lecithin-(PC) from egg yolk (purity > 99%, from Avanti Polar Lipids, Alabaster, AL) and cholesterol (Sigma, St Louis, MO) were dissolved separately in chloroform. The chloroform solutions were then mixed and dried down into a thin film under a stream of nitrogen gas. Residual chloroform was further removed by applying a high vacuum for at least 4 h. The dried thin film was then re-suspended into D_2O and sonicated into vesicles of a mean size of 100–130 nm in diameter.

The noble gas xenon (Linde Specialty Gases, Somerset, NJ) was chosen as an 'unbiased' molecular probe because it is structureless and chemically inert. For each NMR sample, 4 ml of vesicle suspensions were mixed vigorously with 10 ml naturally abundant xenon gas at 1 atm inside a pair of rubber-sealed syringes, and then rapidly injected into a gas-tight, high-precision NMR tube (Wilmad Glass, Buena, NJ) prefilled with naturally abundant xenon gas. To ensure that the final pressure inside the tube was 1 atm, the tube was exposed to 1 atm xenon gas briefly before the gas-tight valve was closed. The samples were allowed to equilibrate at room temperature for at least 2 h before NMR experiments were commenced.

2.2. NMR spectroscopy

All NMR experiments were conducted at 25°C on an Otsuka (Chemagnetics) CMXW-400SLI spectrometer, operating at 110.967 and 401.102 MHz for ^{129}Xe and ^{1}H resonance, respectively. The nominal 90° pulse length for ^{129}Xe was 16 μs. For all ^{129}Xe spectra, 4 scans were summed with a recycle delay of 400 s.

The intermolecular ^{129}Xe-{^{1}H} NOE was measured between ^{129}Xe and the protons in selected regions in the model membrane, using the truncated driven NOE pulse sequence: $P_{t_s}(^{1}H)$-$P_{90°}(^{129}Xe)$-Acq(^{129}Xe)-T_R, where $P_{t_s}(^{1}H)$ was a single or a train of pulses applied to ^{1}H for a period t_s to saturate ^{1}H magnetization. A 90° excitation pulse was then applied to ^{129}Xe, followed by the data acquisition of ^{129}Xe. A recycle

delay of T_R was inserted between repetitive scans to ensure relaxation of ^{129}Xe and ^{1}H magnetization. For the non-selective NOE experiments, in which dynamic polarization transfer was measured from all protons to ^{129}Xe, $P_{t_s}(^1H)$ was a low-power, broadband WALTZ-16 saturation pulse. In selective dynamic polarization transfer experiments, in which only a selected group of protons were saturated, the WALTZ-16 pulse was replaced by a highly frequency-selective, adiabatic pulse train, consisting of low power, 90-ms, hyperbolic secant-shaped inversion pulses [37] interleaved with 10-ms delays. The total ^{1}H saturation time, t_s, was set at seven predetermined values: $t_s = 5$, 20, 40, 70, 100, 150, and 200 s, the order of which was randomized in the experiments. To minimize any unforeseen effects of T_1 relaxation, the T_R was also varied such that $t_s + T_R = c = 400$ s, which is about 6–8-times the T_1 of ^{129}Xe in the lipid vesicle suspension (see below).

2.3. Theoretical analysis of truncated driven, intermolecular NOE

The truncated driven NOE originates from noncoherent nuclear dipole-dipole cross-relaxation and can be analyzed using the classical Solomon equations. For one I spin and N equivalent S spins, these equations are:

$$\frac{dI_z(t)}{dt} = -\rho_I^*\left(I_z(t) - I_z^0\right) - \sum_{i=1}^{N} \sigma_{IS_i}(t)\left(S_z(t) - S_z^0\right)_i \quad (1)$$

$$\frac{dS_{z_i}(t)}{dt} = -\rho_{S_i}^*\left(S_z(t) - S_z^0\right)_i - \sum_{k\neq i} \sigma_{S_iS_k}(t)\left(S_z(t) - S_z^0\right)_k - \sigma_{IS_i}(t)\left(I_z(t) - I_z^0\right) \quad (2)$$

where σ and ρ^* $(= 1/T_{1d\text{-}d})$ are the cross-relaxation and direct dipolar relaxation rates, respectively, the subscripts denote the associated spins, and the superscript 0 indicates the thermal equilibrium state.

In truncated driven NOE, S spins are saturated: $S_{zi}(t) = 0$. For intermolecular dipole–dipole interaction, σ_{ISi} is governed by the intermolecular approaching distance, which varies rapidly with time in the liquid state. By defining a time-averaged intermolecular cross-relaxation rate constant, $<\Sigma\sigma_{ISi}(t)>$, Eq. (1) can be solved to yield:

$$I_z(t_s) = I_z^0 + \frac{\left\langle \sum_{i=1}^{N} \sigma_{IS_i} \right\rangle}{\rho_I^*} S_z^0\left(1 - e^{-\rho_I^* t_s}\right) \quad (3)$$

where t_s is the saturation time for S spins.

The NOE, η, is measured as the relative changes in the I magnetization. Specifically for this study, $I = ^{129}Xe$, $S = ^{1}H$, and the NOE is given by:

$$\eta_{Xe}(t_s) = \frac{\gamma_H}{\gamma_{Xe}} \frac{\left\langle \sum_{i=1}^{N} \sigma_{Xe-H_i} \right\rangle}{\rho_{1_{Xe}}^*}\left(1 - e^{-\rho_{1Xe}^* t_s}\right) \quad (4)$$

where γ_H and γ_{Xe} are gyromagnetic ratios of ^{1}H and ^{129}Xe, respectively. Thus, by measuring η_{Xe} as a function of ^{1}H saturation time (t_s), the ^{129}Xe direct dipolar relaxation rate (ρ_{1Xe}^*) and the time-averaged sum of the cross-relaxation rate constants between ^{129}Xe and the selected ^{1}H $(<\Sigma\sigma_{Xe-Hi}>)$ can be determined.

3. Results

3.1. Non-selective ^{129}Xe-{^{1}H} intermolecular NOE

A strong interaction exists between xenon and the lipid membranes. For ^{129}Xe dissolved in lipid-free D_2O, we found that the T_1 and T_2 of ^{129}Xe, as measured using the conventional inversion-recovery and Carr–Purcell–Meiboom–Gill methods, were 122 ± 37 s (mean ± S.E.) and 17 ± 3 s, respectively. These values were reduced, for example, to 60 ± 14 s and 248 ± 4 ms, respectively, in sonicated PC vesicle suspensions of 37.5 mM lipids without cholesterol, and to 51 ± 4 s and 23 ± 1 ms, respectively, in unsonicated PC suspensions of the same lipid concentration. These reductions resulted primarily from nuclear dipole interaction between ^{129}Xe and protons in the model membrane, as evidenced by the ^{129}Xe-{^{1}H} intermolecular NOE build-up. Fig. 1 shows a representative series of ^{129}Xe-NMR spectra acquired from

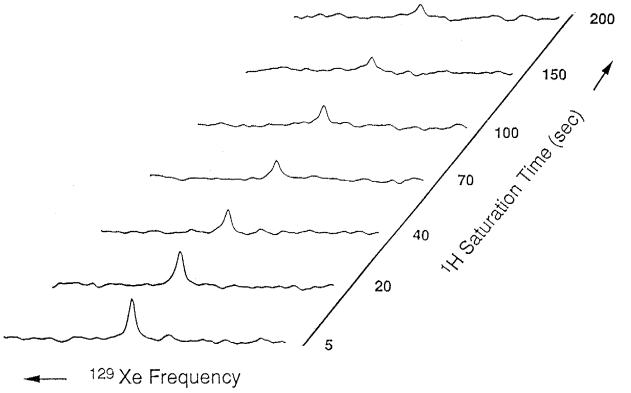

Fig. 1. A series of high-resolution ^{129}Xe-NMR spectra, acquired at nominal clinical concentration of xenon in a liquid suspension of phosphatidylcholine lipid vesicles, are plotted as a function of ^{1}H saturation time, showing non-selective, truncated driven ^{129}Xe-{^{1}H} intermolecular NOE.

naturally abundant xenon ($\approx 26.4\%$ ^{129}Xe) at 1 atm in a D_2O suspension of sonicated PC vesicles (37.5 mM lipids, no cholesterol). After non-selective saturation of ^{1}H, the ^{129}Xe magnetization decreases as a result of negative NOE. (Note that because $\gamma_H/\gamma_{Xe} < 0$, a negative NOE suggests a positive $<\sum\sigma_{Xe\text{-}Hi}>$. See Eq. (4)). The rate of this decrease, measured as a function of the ^{1}H saturation time, can be used to quantify the strength of overall xenon–membrane interaction. For this particular set of spectra, nonlinear least-squares fit using Eq. (4) yields $<\sum\sigma> = 0.163 \pm 0.042$ min^{-1} and $T_{1d\text{-}d} = 71 \pm 10$ s (mean ± S.E.). Placement of saturation frequency outside the ^{1}H spectral width resulted in no change in the ^{129}Xe spectral intensity, confirming that the observed negative NOE was not an artifact.

3.2. Selective ^{129}Xe-{^{1}H} intermolecular NOE

The truncated driven NOE from selected groups of protons in the membrane to ^{129}Xe allows for quantification of specific interaction between xenon and membrane. Our highly frequency-selective pulse train permits selective saturation of individual peaks in the ^{1}H spectra. Examples of excellent spectral selectivity in a sample of 37.5 mM PC (without cholesterol) are shown in Fig. 2a, in which the saturated protons are marked with vertical arrows. Selectivity of the same quality was obtained at all other PC and cholesterol concentrations studied. It is evident from these spec-

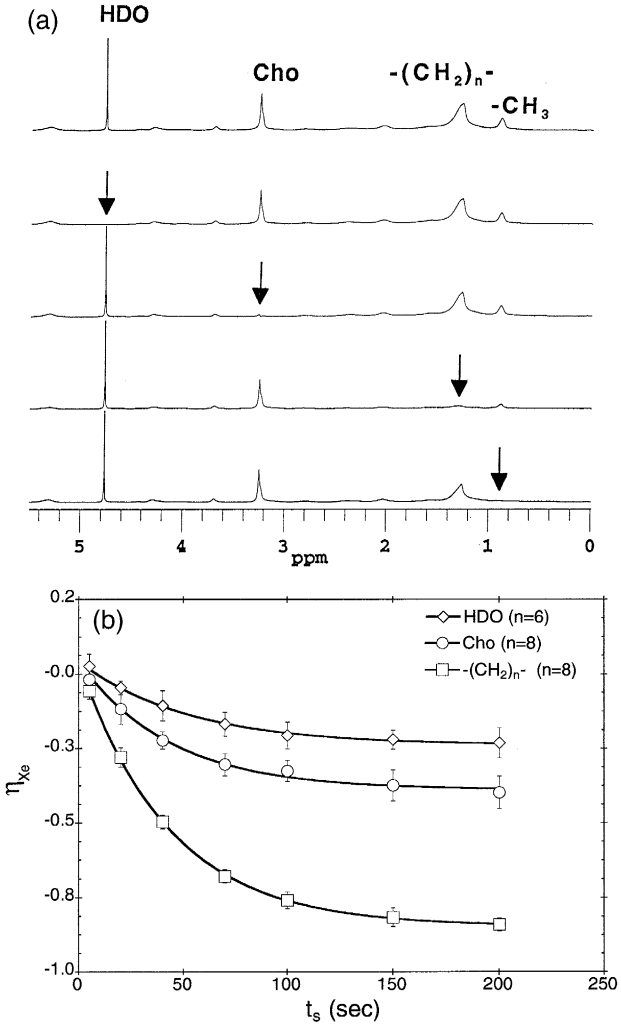

Fig. 2. Selective saturation of a particular group of protons allows for investigation of site-specific ^{129}Xe-^{1}H NOE buildup. (a) Representative ^{1}H-NMR spectra of PC vesicles, showing selective saturation of protons (marked by vertical arrows) in the terminal methyl group ($-CH_3$), the aliphatic methylene group ($(-CH_2)_n$), the choline methyl group (Cho), and the water (HDO), respectively. The top trace is a one-pulse spectrum used as a control. (Data shown are from a sample of 37.5 mM PC without cholesterol. Selectivity is the same at all other PC and cholesterol concentrations studied.) (b) Selective NOEs from $(-CH_2)_n$, Cho, and HDO to ^{129}Xe are measured as a function of ^{1}H saturation time (data shown are from samples of 75 mM lipids without cholesterol). All η_{Xe} values were calculated as relative changes in ^{129}Xe magnetization to its thermal equilibrium value, determined experimentally by placing the saturation pulses outside the ^{1}H spectral bandwidth (1–2 MHz off-resonance). Error bars show the standard deviation (S.D.) of multiple measurements. Solid lines are best fit to the data using Eq. (4), yielding $<\sum\sigma>$ between ^{129}Xe and the three groups of protons (see text for details).

tra that spin diffusion among different groups of protons, a process that would degrade the selectivity, is negligible because the intensities of unsaturated ^{1}H peaks are essentially unchanged. (Exception to this is the saturation of the -CH_3 peak, which severely overlaps with the tail of the broad $(\text{-CH}_2)_n$ peak.) With such selective saturation, NOE from a particular group of protons to ^{129}Xe can be measured based on the resultant change in the ^{129}Xe spectral intensity, similar to that shown in Fig. 1, as a function of ^{1}H saturation time. Representative examples of such measurements at a lipid concentration of 75 mM without cholesterol are shown in Fig. 2b for the aliphatic methylene protons ($(\text{-CH}_2)_n$), the choline methyl protons (Cho), and the water protons (HDO), respectively. The solid lines in Fig. 2b are best fit to the data using Eq. (4), yielding $<\Sigma\sigma_{\text{Xe-CH2}}> = 0.328 \pm 0.004$ min^{-1} (mean ± S.E.), $T_{1\text{d-d}}(\text{Xe-CH}_2) = 43 \pm 1$ s, $<\Sigma\sigma_{\text{Xe-Cho}}> = 0.158 \pm 0.009$ min^{-1}, $T_{1\text{d-d}}(\text{Xe-Cho}) = 44 \pm 3$ s, $<\Sigma\sigma_{\text{Xe-HDO}}> = 0.086 \pm 0.004$ min^{-1}, and $T_{1\text{d-d}}(\text{Xe-HDO}) = 53 \pm 3$ s, where $\sigma_{\text{Xe-CH2}}$, $\sigma_{\text{Xe-Cho}}$, and $\sigma_{\text{Xe-HDO}}$ are the pairwise cross-relaxation rates between ^{129}Xe and the three groups of protons, respectively.

3.3. Pairwise ^{129}Xe-^{1}H cross-relaxation rates

The pairwise cross-relaxation rate, σ, depends on the motional characteristics of the interacting nuclei. A variety of possibilities can be considered, ranging from weak interaction due to translational diffusion of xenon in the vicinity of protons, to tight binding of xenon to protons to form a xenon-membrane complex. In the former extreme, if ^{129}Xe and ^{1}H are approximated by structureless spheres, then σ can be shown to be proportional to the concentration of the protons causing the relaxation, and inversely to the distance of closest approach and the mutual (translational) self-diffusion constant of xenon and lipid molecules [38]. In the latter extreme, where the interaction can be viewed as intramolecular, σ is proportional to the correlation time of xenon-membrane complex (assuming extreme narrowing condition) and inversely to the sixth power of the internuclear distances [39]. Situations intermediate to these extremes are likely to occur under normal experimental conditions, and are often too complicated to be examined analytically.

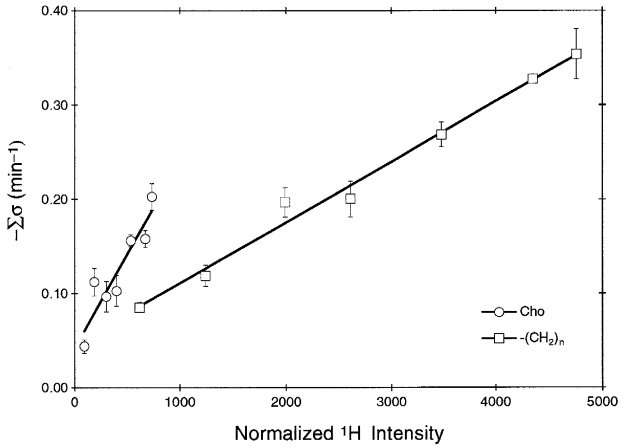

Fig. 3. $<\Sigma\sigma_{\text{Xe-Cho}}>$ and $<\Sigma\sigma_{\text{Xe-CH2}}>$ are plotted as a function of normalized ^{1}H peak intensity when the lipid concentration increases from 11 to 82 mM (no cholesterol). Error bars indicate ± S.D. ($n = 4$). The solid lines are linear least-squares fit to the data. The linear increase in $<\Sigma\sigma>$ suggests that $<\Sigma\sigma>$ is proportional to the number of protons contributing to the selective NOE. The proportionality (the slope) is a measure of the mean pairwise cross-relaxation rate, $<\sigma>$.

For simplicity, we assume that a mean pairwise cross-relaxation rate, $<\sigma>$, can be defined between ^{129}Xe and ^{1}H such that $<\sigma>$ is identical for all protons in the same group. Thus, $<\Sigma\sigma> = N_k \times <\sigma>$, where N_k is the number of protons in group k. When the lipid concentration increases, N_k increases proportionally and so does the NMR peak intensity for the corresponding ^{1}H group. Fig. 3 depicts $<\Sigma\sigma>$ as a function of normalized ^{1}H intensities for Cho and $(\text{-CH}_2)_n$ when lipid concentration is varied from 11 to 82 mM (no cholesterol). Each point in this figure resulted from fittings of repeated NOE measurements, similar to that shown in Fig. 2b, at the given PC concentrations. Solid lines are linear least-squares fit to the data, yielding slopes proportional to $<\sigma>$ of the two ^{1}H groups. From Fig. 3, it is evident that the mean pairwise cross-relaxation rate between xenon and the Cho group in the lipid head region is at least three times greater than that between xenon and the aliphatic methylene group mostly in the tail region (i.e., $<\sigma_{\text{Xe-Cho}}> : <\sigma_{\text{Xe-CH2}}> \geq 3{:}1$). Because mean pairwise $<\sigma>$ reflects the closeness and tightness of xenon–proton interaction, a larger $<\sigma_{\text{Xe-Cho}}>$ compared to $<\sigma_{\text{Xe-CH2}}>$ suggests that a strong xenon–membrane interaction is directed to-

ward the amphiphilic head region of the lipids, rather than to the lipophilic tail region.

3.4. Involvement of interfacial water in xenon–membrane interaction

The presence of lipid vesicles can enhance the xenon–water interaction, which seems to occur at the lipid/water interface. In lipid-free bulk water, the pairwise cross-relaxation between ^{129}Xe and water proton was negligibly weak. No NOE build-up was measurable between ^{129}Xe and HDO in bulk D_2O, and a summation over ≈ 28 M of water protons (i.e., 25% H_2O in D_2O) yields only a $<\Sigma\sigma>$ of 0.072 $\pm$ 0.012 min^{-1}. This changed, however, when lipids were present. We found that $<\Sigma\sigma_{\text{Xe-HDO}}>$ increased linearly with increasing lipid concentrations. For lipid concentrations in the range of 11 to 82 mM (i.e., the same range as that shown in Fig. 3), $<\Sigma\sigma_{\text{Xe-HDO}}>$ increases from 0.049 ± 0.007 to 0.129 ± 0.010 min^{-1}. We believe that this increase is related to the increase in total vesicle surface area and therefore represents xenon–water interaction at the lipid/water interface. The possibility of unforeseen lipid saturation can be ruled out because the $T_{1d\text{-}d}$ associated with $<\Sigma\sigma_{\text{Xe-HDO}}>$ is at least 20% longer than that associated with $<\Sigma\sigma_{\text{Xe-CH2}}>$ or $<\Sigma\sigma_{\text{Xe-Cho}}>$, and because selective irritation in the vicinity of the water peak (about $\pm$ 100 Hz off resonance) resulted in smaller $<\Sigma\sigma_{\text{Xe-HDO}}>$ due to partial HDO saturation. The latter would not be expected if $<\Sigma\sigma_{\text{Xe-HDO}}>$ were originated from saturation of an NMR-invisible broad component.

3.5. Effects of cholesterol on ^{129}Xe-{^{1}H} NOE

The tendency of xenon to interact favorably with the interfacial region of the lipid vesicle is enhanced with increasing cholesterol concentrations. Addition of cholesterol to the lipid bilayer caused a linear increase in $<\Sigma\sigma>$, as shown in Fig. 4, but to a different extent depending on the specific proton groups. Thus, at a fixed PC concentration of 45.0 mM and for an increase from 0 to 50% (mol/mol) in cholesterol concentration, $<\Sigma\sigma_{\text{Xe-Cho}}>$ increased by $\approx 120\%$, $<\Sigma\sigma_{\text{Xe-HDO}}>$ by $\approx 118\%$, and $<\Sigma\sigma_{\text{Xe-CH2}}>$ by only $\approx 20\%$. The increase in $<\Sigma\sigma_{\text{Xe-CH2}}>$ is smaller than what would be expected for the increase in the number of protons attributable to cholesterol in the $(\text{-CH}_2)_n$ and -CH_3 regions, suggesting that cholesterol either has no effect on the mean pairwise cross-relaxation rate in this region, or actually reduces it. In contrast, because no resonance from cholesterol overlaps with the Cho peak (thus the number of protons in this group is constant), the significant increase in $<\Sigma\sigma_{\text{Xe-Cho}}>$ after addition of cholesterol is entirely due to increase in mean pairwise $<\sigma_{\text{Xe-Cho}}>$ (i.e., stronger Xe–Cho interaction). This result is consistent with the finding from other methods [40–43] that cholesterol rigidifies the head region of the bilayer; a reduction in mobility in the head region enhances the mean cross-relaxation rate $<\sigma_{\text{Xe-Cho}}>$. The effects of cholesterol on $<\Sigma\sigma_{\text{Xe-HDO}}>$ are twofold. On the one hand, cholesterol is known to reduce the number of hydration (from 22 to 8 or 9 per lipid molecule, [43]) and therefore reduce the number of water protons interacting with xenon at the interface. On the other hand, the interfacial hydroxyl protons of the cholesterol resonate at the same frequency as those of water and therefore also contributes to $<\Sigma\sigma_{\text{Xe-HDO}}>$. Although the loss of interfacial water protons outnumbers the gain of cholesterol hydroxyl protons, an increase in $<\Sigma\sigma_{\text{Xe-HDO}}>$ by 118% strongly indi-

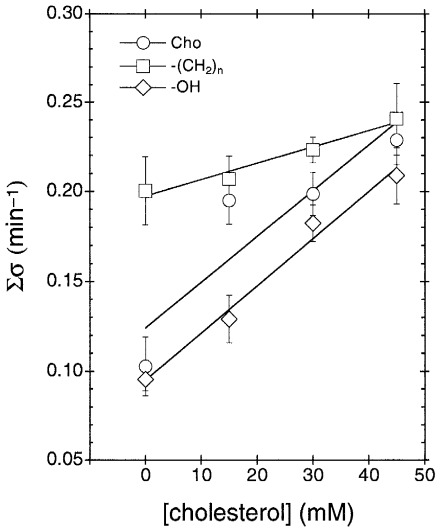

Fig. 4. Dependence of $<\Sigma\sigma>$ on cholesterol concentration. The PC concentration was constant (45.0 mM). Error bars show $\pm$S.D. ($n = 4$). The solid lines are linear least-squares fit to the data.

cates that cholesterol significantly augments $<\sigma_{\text{Xe-HDO}}>$, mostly due to xenon interaction with the cholesterol's hydroxyl protons at the lipid/water interface. Because the cholesterol-to-lipid ratio in the central nervous system is typically 40% (mol/mol) [44], xenon interaction with neuronal membranes in vivo is likely to be directed toward the head and interfacial region, more so than indicated in Fig. 3.

4. Discussion

The tendency for xenon to interact preferably with the amphiphilic interface of the lipid vesicles over the more lipophilic tail region and the more hydrophilic aqueous region has significant implications. It not only provides direct experimental evidence to support the possibility of amphiphilic sites for anesthetic action, but also explains why for many volatile anesthetics, the product of potency × oil/gas partition coefficient deviates more from a constant predicted by the Meyer–Overton rule [45] than does the product of potency × oil/gas partition coefficient × saline/gas partition coefficient [23]. (The second product clearly implicates the importance of a polar component.) More importantly, our results show that the selection of molecular target sites, when many different types are available, depends not only on the properties of the anesthetic molecule itself, but also on possible changes in these properties after interaction with a membrane takes place. Thus, although xenon is apolar (with a spherical symmetry) in the gas phase and would be expected to be more compatible with the core of the lipid bilayer, its choice for the interface is clearly governed, once in the membrane, by the *induced* dipole that makes xenon more adaptable to an amphiphilic region. A similar but opposite argument could be made that some molecules, having a 'desirable' solubility in olive oil to be anesthetics according to the Meyer–Overton rule, find themselves attractable to the more lipophilic core of the lipid after dissolving into the membrane and henceforth become nonanesthetics. A generalization of this would suggest that molecules that are amphiphilic after interacting with membrane constituents are anesthetics, whereas those that are either extremely lipophilic or extremely hydrophilic are likely to have minimal or no anesthetic effects. If this is true, then it is not surprising that disobedience to Meyer–Overton rule occurs.

The involvement of a polar component in anesthetic action has been postulated previously. Theoretically, it has been predicted [46,47] that polar interactions like the breaking and formation of hydrogen bonds are important for the mechanisms of general anesthesia, and that the polarizability of a nonpolar molecule may be relevant to its anesthetic effect. Experimentally, it has been shown that anesthetic alcohols can bind to the surface of dimyristoylphosphatidylcholine (DPPC) membranes [48,49], release water molecules from the lipid surface [22,50,51], and produce stronger effects on the pretransition temperature (which is believed to relate to the hydrophilic head property) than on the main transition temperature of a membrane [52]. In a recent two-dimensional ^{1}H NOESY study using high concentration of methoxyflurane in DPPC vesicles [53], a pair of cross peaks was detected between the choline methyl protons of the DPPC and the methoxy protons of the methoxyflurane. No other cross peaks were found. Based on these results, it has been suggested [53] that the probability of finding anesthetic molecules is highest at the lipid interface.

It should be noted that our choice of PC lipids as a model was arbitrary. Amphiphilic domains exist also in neuronal proteins. A superfamily of neurotransmitter-gated receptor channels, including the γ-aminobutyric acid type A receptor, the glycine receptor, the nicotinic acetylcholine receptor, and 5-hydroxytryptamine type 3 receptor, are particularly sensitive to general anesthetics [9,54]. The subunits of these receptors have similar overall hydrophobicity and hydrophilicity pattern that fluctuates along the sequence between lipophilic and hydrophilic extremes [55]. Such fluctuation may result in residues with amphiphilic characteristics. Therefore, a plausible mechanism of general anesthetic action is to nonspecifically alter the amphiphilic domains in these receptors such that association of the receptor with the aqueous environment at the membrane interface is changed. This change, in turn, may cause alteration in receptor conformation or agonist affinity to the receptor binding sites, or both.

In conclusion, a chemically and structurally unbiased general anesthetic was found to interact prefer-

entially with the amphiphilic region of a model biomembrane.

Acknowledgements

We thank Dr. Leonard Firestone for suggestions and discussion and Dr. Peter M. Winter for encouragement and support. This work was supported by grants from the National Institutes of Health (GM49202) and from University Anesthesiology and Critical Care Medicine Foundation, University of Pittsburgh.

References

[1] Miller, K.W. (1985) Int. Rev. Neurobiol 27, 1–61.
[2] Ueda, I., Chiou, J.S., Krishna, P.R. and Kamaya, H. (1994) Biochim. Biophys. Acta 1190, 421–429.
[3] Ueda, I., Tatara, T., Chiou, J.S., Krishna, P.R. and Kamaya, H. (1994) Anesth. Analg. 78, 718–725.
[4] Forman, S.A. and Miller, K.W. (1989) Trends Pharmacol. Sci. 10, 447–452.
[5] Bangham, A.D. and Hill, M.W. (1986) Chem. Phys. Lipids 40, 189–205.
[6] Raines, D.E. and Cafiso, D.S. (1989) Anesthesiology 70, 57–63.
[7] Gruner, S.M. and Shyamsunder, E. (1991) Ann. NY Acad. Sci. 625, 685–697.
[8] Trudell, J.R. (1977) Anesthesiology 46, 5–10.
[9] Franks, N.P. and Lieb, W.R. (1994) Nature 367, 607–614.
[10] Franks, N.P. and Lieb, W.R. (1990) Environ. Health Perspect. 87, 199–205.
[11] Franks, N.P. and Lieb, W.R. (1987) Trends Pharmacol. Sci. 8, 169–174.
[12] Forman, S.A., Miller, K.W. and Yellen, G. (1995) Mol. Pharmacol. 48, 574–581.
[13] Ueda, I. (1995) Masui 44, 480–488.
[14] Meyer, H.H. (1899) Arch. Exp. Pathol. Pharmakol. 42, 109–118.
[15] Overton, C.E. (1901) Studien uber Narkose, zugleich ein Beitrag zur allgemeinen Pharmakologie, Fisher, Jena.
[16] Franks, N.P. and Lieb, W.R. (1984) Nature 310, 599–601.
[17] Alifimoff, J.K., Firestone, L.L. and Miller, K.W. (1987) Anesthesiology 66, 55–59.
[18] Raines, D.E., Korten, S.E., Hill, A.G. and Miller, K.W. (1993) Anesthesiology 78, 918–927.
[19] Liu, J., Laster, M.J., Koblin, D.D., Eger, E.I., II, Halsey, M.J., Taheri, S. and Chortkoff, B. (1994) Anesth. Analg. 79, 238–244.
[20] Liu, J., Laster, M.J., Taheri, S., Eger, E.I., II, Koblin, D.D. and Halsey, M.J. (1993) Anesth. Analg. 77, 12–18.
[21] Koblin, D.D., Chortkoff, B.S., Laster, M.J., Eger, E.I., II, Halsey, M.J. and Ionescu, P. (1994) Anesth. Analg. 79, 1043–1048.
[22] Chiou, J.S., Ma, S.M., Kamaya, H. and Ueda, I. (1990) Science 248, 583–585.
[23] Liu, J., Laster, M.J., Taheri, S., Eger, E.I., II, Chortkoff, B. and Halsey, M.J. (1994) Anesth. Analg. 79, 1049–1055.
[24] Requena, J., Velaz, M.E., Guerrero, J.R. and Medina, J.D. (1985) J. Membr. Biol. 84, 229–238.
[25] Taheri, S., Laster, M.J., Liu, J., Eger, E.I., II, Halsey, M.J. and Koblin, D.D. (1993) Anesth. Analg. 77, 7–11.
[26] Chortkoff, B.S., Laster, M.J., Koblin, D.D., Taheri, S., Eger, E.I., II and Halsey, M.J. (1994) Anesth. Analg. 79, 234–237.
[27] Raines, D.E. and Miller, K.W. (1994) Anesth. Analg. 79, 1031–1033.
[28] Boomsma, F., Rupreht, J., Man in 't Veld, A.J., de Jong, F.H., Dzoljic, M. and Lachmann, B. (1990) Anaesthesia 45, 273–278.
[29] Burov, N.E., Kornienko, L., Dzhabarov, D.A., Mironova, I.I., Morozova, V.T., Ageeva, L.A., Ostapchenko, D.A. and Shulunov, M.V. (1993) Anesteziol. Reanimatol., 14–18.
[30] Burov, N.E., Dzhabarov, D.A., Ostapchenko, D.A., Kornienko, L. and Shulunov, M.V. (1993) Anesteziol. Reanimatol., 7–11.
[31] Kennedy, R.R., Stokes, J.W. and Downing, P. (1992) Anaesth. Intensive Care 20, 66–70.
[32] Lachmann, B., Armbruster, S., Schairer, W., Landstra, M., Trouwborst, A., Van, D.G., Kusuma, A. and Erdmann, W. (1990) Lancet 335, 1413–1415.
[33] Xu, Y. and Tang, P. (1994) in Book of Abstracts, 35th Experimental NMR Conference, Vol. 1, pp. 62, Pacific Grove, CA.
[34] Tang, P. and Xu, Y. (1994) Anesthesiology 81, A413.
[35] Xu, Y. and Tang, P. (1995) in Book of Abstracts, Int. Soc. Magnet. Reson. Med., Vol. 1, pp. 152, Nice, France.
[36] Smith, R.A., Porter, E.G. and Miller, K.W. (1981) Biochim. Biophys. Acta 645, 327–338.
[37] Silver, M.S., Joseph, R.I., Chen, C.N., Sank, V.J. and Hoult, D.I. (1984) Nature 310, 681–683.
[38] Noggle, J.H. and Schirmer, R.E. (1971) in The Nuclear Overhauser Effect: Chemical Applications, pp. 31–34, Academic Press, New York.
[39] Macura, S. and Ernst, R.R. (1980) Mol. Phys. 41, 95–117.
[40] Robinson, A.J., Richards, W.G., Thomas, P.J. and Hann, M.M. (1995) Biophys. J. 68, 164–170.
[41] Morrow, M.R., Singh, D.M. and Grant, C.W. (1995) Biophys. J. 69, 955–964.
[42] Morrow, M.R., Singh, D., Lu, D. and Grant, C.W. (1995) Biophys. J. 68, 179–186.
[43] Faure, C., Tranchant, J.F. and Dufourc, E.J. (1996) Biophys. J. 70, 1380–1390.
[44] Dickinson, R., Franks, N.P. and Lieb, W.R. (1994) Biophys. J. 66, 2019–2023.
[45] Taheri, S., Halsey, M.J., Liu, J., Eger, E.I., II, Koblin, D.D. and Laster, M.J. (1991) Anesth. Analg. 72, 627–634.

[46] Hobza, P., Mulder, F. and Sandorfy, C. (1981) J. Am. Chem. Soc. 103, 1360–1366.
[47] Hobza, P., Mulder, F. and Sandorfy, C. (1982) J. Am. Chem. Soc. 104, 925–928.
[48] Katz, Y. and Diamond, J.M. (1974) J. Membr. Biol. 17, 101–120.
[49] Diamond, J.M. and Katz, Y. (1974) J. Membr. Biol. 17, 121–154.
[50] Chiou, J.S., Kuo, C.C., Lin, S.H., Kamaya, H. and Ueda, I. (1991) Alcohol 8, 143–150.
[51] Chiou, J.S., Krishna, P.R., Kamaya, H. and Ueda, I. (1992) Biochim. Biophys. Acta 1110, 225–233.
[52] Veiro, J.A., Nambi, P., Herold, L.L. and Rowe, E.S. (1987) Biochim. Biophys. Acta 900, 230–238.
[53] Yokono, S., Ogli, K., Miura, S. and Ueda, I. (1989) Biochim. Biophys. Acta 982, 300–302.
[54] Wood, S.C., Tonner, P.H., De Armendi, A.J., Bugge, B. and Miller, K.W. (1995) Mol. Pharmacol. 47, 121–130.
[55] Claudio, T., Ballivet, M., Patrick, J. and Heinemann, S. (1983) Proc. Natl. Acad. Sci. USA 80, 1111–1115.